

Medical Image Enhancement Based On Wavelet Transform

Chintada Lavanya¹, D. Yugandhar²

¹M.Tech (DECS), AITAM, Tekkali

²Assoc Prof. ECE, AITAM, Tekkali

Abstract: Medical Images are often degraded by electronic equipments, power fluctuations and surrounding environment conditions. Medical images are widespread use in the detection of numerous diseases but noise and blurs present in medical images create obstacles in diagnose diseases. In this paper, Blind Image De-convolution (BID) procedure is implemented to restore mammographic images from Gaussian blur and then enhancement process is done using real dual tree wavelet transform. The result of these methods is also compared with the hybrid combination of BID, conventional wavelet Transform and median filter approach to remove Gaussian noise, Salt & Pepper and Speckle Noise with Gaussian blur. Mini-MIAS database is considered to evaluate the performance of these techniques.

Keywords: Mammographic Image, Blur & Noise, BID, Real Dual Tree Wavelet Transform

I. Introduction

Image Processing is a technique to enhance raw images received from cameras/sensors placed on satellites, space probes and aircrafts or pictures taken in normal day-to-day life for various applications. Image de-noising is a technique which removes out noise which is added in the original image. Noise reduction is an important part of image processing systems. An image is always affected by noise. In recent years, the demand for resolution enhancement of pictorial data in medical images has been increased in order to assist clinicians to make accurate diagnosis. The medical image plays an important role in the clinical diagnosis and therapy of doctor and teaching and researching. Medical imaging always appears low image quality caused by fairly low spatial resolution and the presence of noise [1]-[4].

Image Restoration plays an important role in medical image processing. The main objective of Image Restoration is to recover the original image from a degraded image which is blurred by a degradation function, commonly by a Point Spread Function (PSF). Image restoration is a process of increasing the quality of the degraded image. Image restoration techniques are divided in to two broad categories: Image De-convolution and Blind Image De-convolution. Image De-convolution is a linear image restoration problem where the parameters of the true image are estimated using the observed or degraded image and a known Point Spread Function(PSF)[5]. BID is a different approach to image restoration as it is performed with no prior knowledge of the degrading function as well as noise[6].

Medical image enhancement techniques are important methods to increase qualities of image processing results. They often used to improve the useful information in an image for diagnosis purposes because medical image qualities are often deteriorated by noise and other data acquisition devices, illumination conditions, etc. The aims of medical image enhancement are mainly to increase low contrast and reduce the high level noises. Medical image enhancement algorithms have been studied mainly on grayscale transform and frequency domain transform. The image enhancement algorithms based on the wavelet transform are typical method in the frequency domain approaches. Wavelet transform is the improved version of Fourier transform. While Fourier transform is a powerful tool for analyzing the components of a stationary signal, it fails for analyzing the non-stationary signal whereas wavelet transform allows the components of a non-stationary signal to be analyzed. Wavelet transforms have shown promising results for localization in both time and frequency, and hence have been used for image processing applications including noise removal [7-8].

II. Medical Imaging

Medical imaging is concerned with the development of the imaging devices that help to identify different aspects of the tissue and organs based on various properties and reveal new properties of the tissue and internal structure. Medical image processing is a field of science that is gaining wide acceptance in healthcare industry due to its technological advances and software breakthroughs. It plays a vital role in disease diagnosis and in improved patient care. It also helps medical practitioners during decision making with regard to the type of treatment. Medical images include images like mammographic images, X-ray images, ultrasound images and many more [9]. Unfortunately, in spite of highly technical machines, medical images are not acquired properly; they are somewhat unclear or blurred. Blind Image De-convolution is a technique of image restoration which is applied in various fields. BID has been successively used to restore the images related to medical science. To

detect various kinds of diseases, medical science uses medical images. The restoration of ultrasound imaging has been intensively considered after Jensen introduced a convolution model from the standard wave equation using the first-order born approximation [10]. The ultrasound pulse is the single system input and tissue reflectivity functions are the channel impulse responses [11]. Masahiro Kido developed an image restoration method which removed a blur by estimating PSF on chest X-ray photography using Iterative Blind Deconvolution [12].

A. Mammographic Images

Mammographic images are obtained in the process of mammography. Mammography is the process of using low energy X-rays to examine the human breast and is used as a diagnostic and a screening tool. The goal of mammography is the early detection of breast cancer, typically through detection of characteristic masses and micro calcifications. Fig 1. Shows mammographic image.

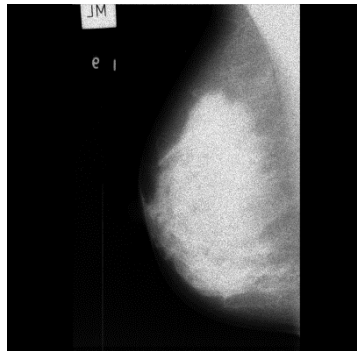


Fig 1: Mammographic image

Mammographic images have low image duality caused by fairly low spatial resolution and the presence of noise. Hence restoration of mammographic images is very challenging. Mencattini presented an algorithm for mammographic images enhancement and de-noising based on the wavelet transform in the year 2006[13].A number of comparison works have also been done in this field using different types of filters depending upon different types of noises present in the mammographic images[14].

III. Blind Image Deconvolution

Blind image de-convolution is a technique of image restoration which restores the degraded image that is blurred by an unknown PSF. It is a de-convolution technique that permits recovery of the target image from a single or set of blurred images in the presence of a poorly determined or unknown PSF. In this technique firstly, we have to make an estimate of the blurring operator i.e. PSF and then using that estimate we have to deblur the image. This method can be performed iteratively as well as non-iteratively. In iterative approach, each iteration improves the estimation of the PSF and by using that estimated PSF we can improve the resultant image repeatedly by bringing it closer to the original image. In non-iterative approach one application of the algorithm based on exterior information extracts the PSF and this extracted PSF is used to restore the original image from the degraded one. The Fig 2 shows the image restoration using blind deconvolution.

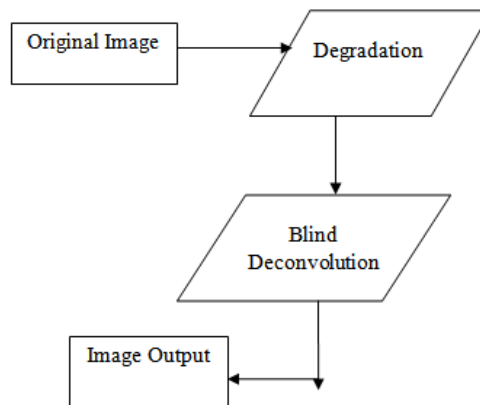


Fig 2: Image restoration using blind de-convolution

IV. Wavelets

Wavelet is nothing but a small wave of varying frequency and limited duration. Wavelet can also be said as an oscillation that decays speedily. Wavelets are the foundation for representing images in various degrees of resolution. This is used for image data compression and for pyramidal representation, in which images are subdivided successfully in to smaller regions. The imaging applications from a wavelet point of view include image matching, segmentation, de-noising, restoration, enhancement, compression, and other medical image technologies, etc. The term “wavelet” was introduced by Morlet [15]. Later, Mallat [16] proposed the fast wavelet transform. Wavelet denotes a function defined on \mathbb{R} , which, when subjected to the fundamental operations of shifts (*i.e.*, translation by integers) and dyadic dilation, yields an orthogonal basis of $L^2(\mathbb{R})$. That is, the wavelet series expansion of function (x) relative to scaling function (x) and wavelet function (x) are defined by Eq. (1).

$$f(x) = \sum_k c_{j_0}(k)\varphi_{j_0,k}(x) + \sum_{j=j_0}^{\infty} \sum_k d_j(k)\psi_{j,k}(x) \tag{1}$$

Where, j_0 is an arbitrary starting scale. Also $c_{j_0}(k)$ is called the scaling coefficients and $d_j(k)$ is referred to as the detail or wavelet coefficients. The expansion of coefficients is calculated as in Eq. (2) and Eq. (3).

$$c_{j_0}(k) = \langle f(x), \varphi_{j_0,k}(x) \rangle = \int f(x)\varphi_{j_0,k}(x)dx \tag{2}$$

and

$$d_j(k) = \langle f(x), \psi_{j,k}(x) \rangle = \int f(x)\psi_{j,k}(x)dx \tag{3}$$

The Wavelet Series is just a sampled version of Continuous Wavelet Transform (CWT) and its computation may consume significant amount of time and resources, depending on the resolution required. If the function being expanded is a sequence of numbers, like samples of a continuous function $f(x)$, the resulting coefficients are called the Discrete Wavelet Transform (DWT) of $f(x)$. In this case, the series expansion of wavelet transform in one dimension is of two sequences are expressed in Eq. (4) and Eq. (5) respectively.

$$W_{\varphi}(j,k) = \frac{1}{\sqrt{M}} \sum_x f(x)\varphi_{j_0,k}(x) \tag{4}$$

$$W_{\psi}(j,k) = \frac{1}{\sqrt{M}} \sum_x f(x)\chi_{j_0,k}(x) \tag{5}$$

For $j \geq j_0$ and the total wavelet sequence can be written as equation (6),

$$f(x) = \frac{1}{\sqrt{M}} \sum_k W_{\varphi}(j,k)\varphi_{j_0,k}(x) + \frac{1}{\sqrt{M}} \sum_{j=j_0}^{\infty} \sum_k W_{\psi}(j,k)\chi_{j,k}(x) \tag{6}$$

Here, $f(x)$, $\varphi_{j_0,k}(x)$, and $\psi_{j,k}(x)$ are functions of the discrete variable $x=0,1,2,\dots,M-1$.

An obvious way to extend Discrete Wavelet Transform (DWT) to the 2-D case is to use separable wavelets obtained from 1-D wavelets. One-level 2-D DWT of an $N \times N$ image can be implemented using 1-D DWT along the rows, leading to two sub-images of size $N/2 \times N$, followed by 1-D DWT along the columns of these two images, resulting in four sub-images of size $N/2 \times N/2$. Fig 3. Shows this process. The first sub-image obtained by low-pass filtering and sub sampling along rows and columns gives the low-pass approximation (LL), and the second one obtained by low-pass filtering and sub sampling along rows and high-pass filtering and sub sampling along columns gives the first added details corresponding to the vertical edge details (LH), and the third and fourth ones similarly give the horizontal (HL) and diagonal edge details (HH). Reconstruction from these sub-images can be done similar to the 1-D case. The process can be iterated on the low-pass approximation several times as in the 1-D case to obtain finer frequency resolution and perform multi-level 2-D DWT.

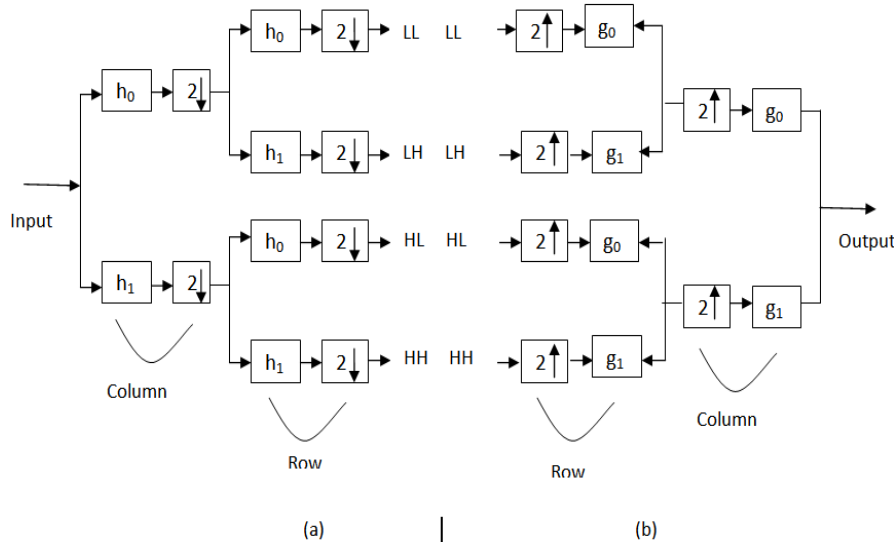


Fig 3: Discrete Wavelet Transform. (a) Decomposition (b) Reconstruction.

A. Dual Tree Discrete Wavelet Transform

The dual-tree complex DWT of a image x is implemented using two critically-sampled DWTs in parallel on the same data as shown in the Fig 4.

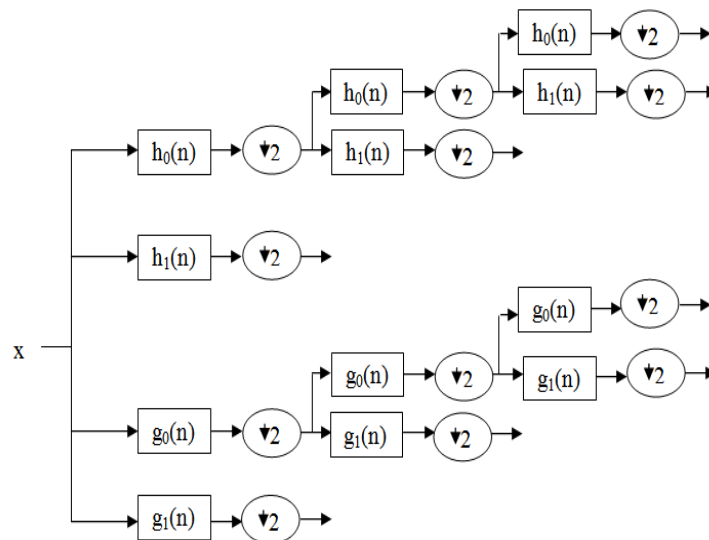


Fig 4: 2-D Dual Tree Discrete Wavelet Transform

This transform is 2-times expansive because for an N -point signal it gives $2N$ DWT coefficients. If the filters in the upper and lower DWTs are the same, then no advantage is gained. However, if the filters are designed in a specific way, then the sub band signals of the upper DWT can be interpreted as the real part of a complex wavelet transform, and sub band signals of the lower DWT can be interpreted as the imaginary part. The dual-tree complex DWT can be used to implement wavelet transforms where each wavelet is oriented, which is especially useful for image processing. For the separable DWT, recall that one of the three wavelets does not have a dominant orientation. There are two types of the 2-D dual-tree wavelet transform: the real dual-tree DWT and complex 2-D dual tree DWT.

B. Real Dual-Tree Discrete Wavelet Transform (RDTWT)

The real dual-tree DWT of an image X is implemented using two critically-sampled separable DWTs in parallel. Then for each pair of sub bands we take the sum and difference.

V. Proposed Method

The block diagram representation of proposed method is shown in Fig 5.

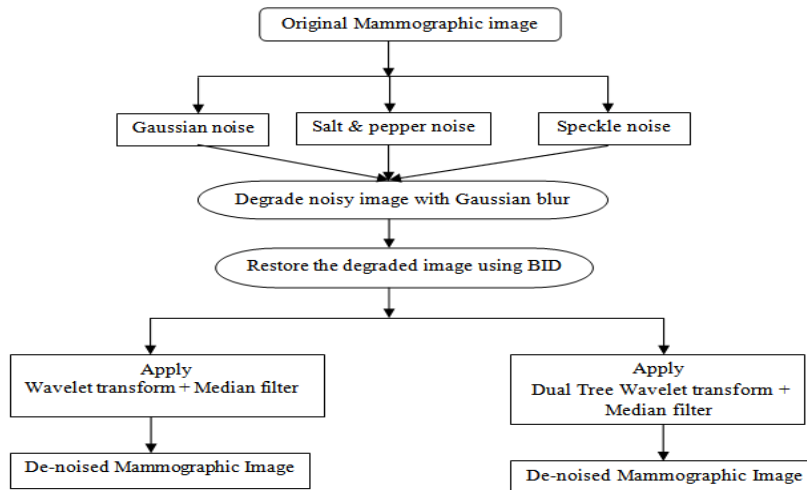


Fig 5: Block diagram of Proposed Method

In order to reduce noise or to de-noise the image, the following steps are involved. They are:

- Step 1: Read the original mammographic image.
- Step 2: Add Gaussian noise with mean zero and variance 0.01, Salt & pepper noise with density 10%, Speckle noise with variance 0.01.
- Step 3: Add Gaussian blur to the noisy image.
- Step 4: The degraded image is restored using the Blind Image De-convolution (BID).
- Step 5: The conventional Wavelet transform and Median filter is applied for the restored image.
- Step 6: The Real Dual Tree Wavelet transform (RDTWT) and Median filter is applied for step 4.
- Step 7: By changing the step 2 with same mean and variance 0.02, Salt & pepper noise with density 20%, Speckle noise with variance 0.02. Repeat the step 3, 4, 5 and 6.
- Step 8: Repeat the step 7 with mean zero and variance 0.03, Salt & pepper noise with density 30%, Speckle noise with variance 0.03.
- Step 9: De-noise the mammographic image.

Performance of the proposed work is evaluated using three performance parameters namely Peak Signal to Noise Ratio(PSNR) which is used to measure noise reduction, Mean Squared Error(MSE) and Mean Absolute Error(MAE). The Mean Squared Error (MSE) of two monochromes images is given Eq. (5).

$$MSE = \frac{\sum_i \sum_j (X_{ij} - R_{ij})^2}{M * N} \tag{5}$$

The Mean Absolute Error (MAE) is defined Eq. (6).

$$MAE = \frac{1}{mn} \sum_{i=0}^{M-1} \sum_{j=0}^{N-1} (X(i, j) - R(i, j)) \tag{6}$$

The Peak Signal to Noise Ratio (PSNR) is defined Eq. (7).

$$PSNR = 10 \log_{10} (255^2 / MSE) \tag{7}$$

Where,

X - Original Image, R - de-noised Image, M x N - Size of Image. I, j –coordinates of image.

VI. Results

With the help of various performance parameters the performance of the BID technique is evaluated. Fig 6. Shows the original image.

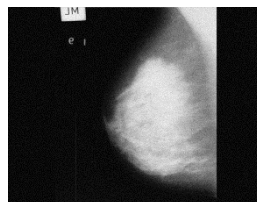


Fig 6: Original Image

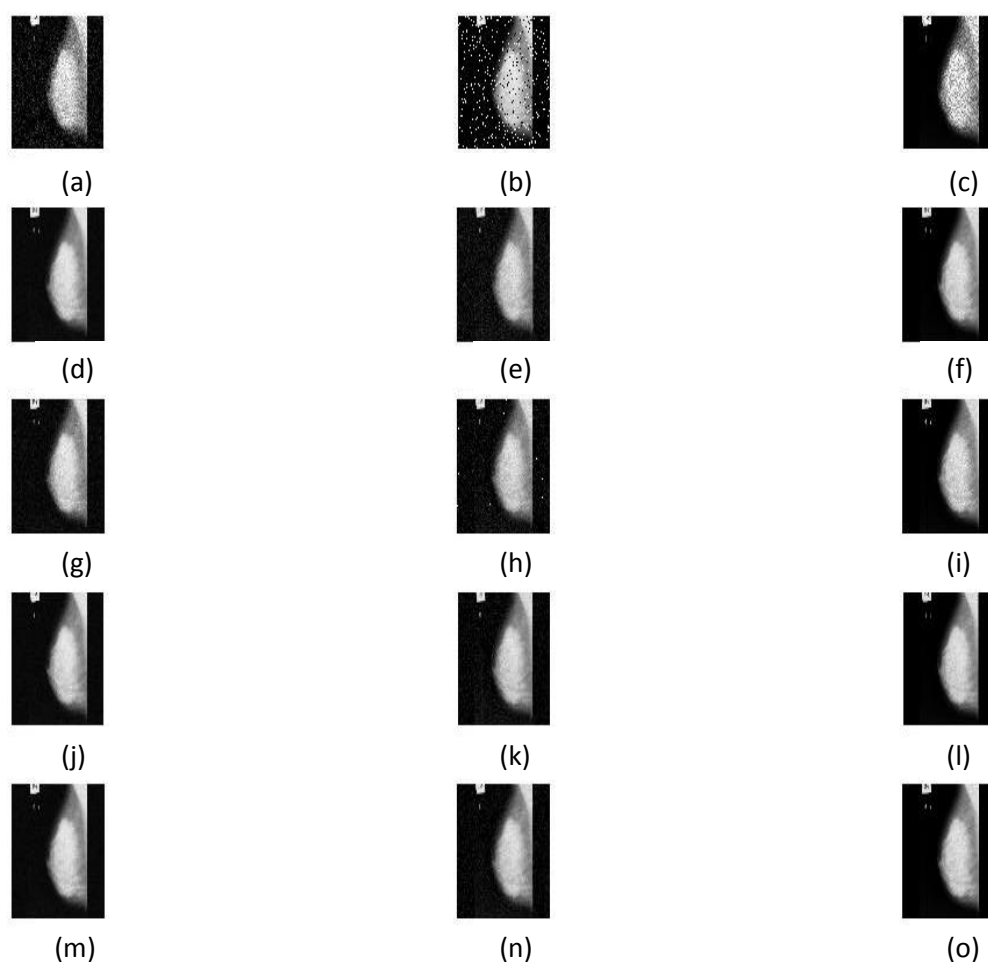


Fig 7: (a) Gaussian noise image with mean zero and variance 0.01 (b) Salt &pepper noise image With density 10% (c) Speckle noise image with variance 0.04 (d) Gaussian noise with blur (e) Salt &pepper noise with blur (f) Speckle noise with blur (g) Restored image of fig (a). (h) Restored image of fig (b). (i) Restored image of fig (c). (j) Wavelet transforms and Median filter is applied to fig (g). (k) Wavelet transforms and Median filter is applied to fig (h). (l) Wavelet transform and Median filter is applied to fig (i). (m) RDTWT an Median filter is applied to fig (g). (n) RDTWT and Median filter is applied to fig (h). (o) RDTWT and Median filter is applied to fig (i).

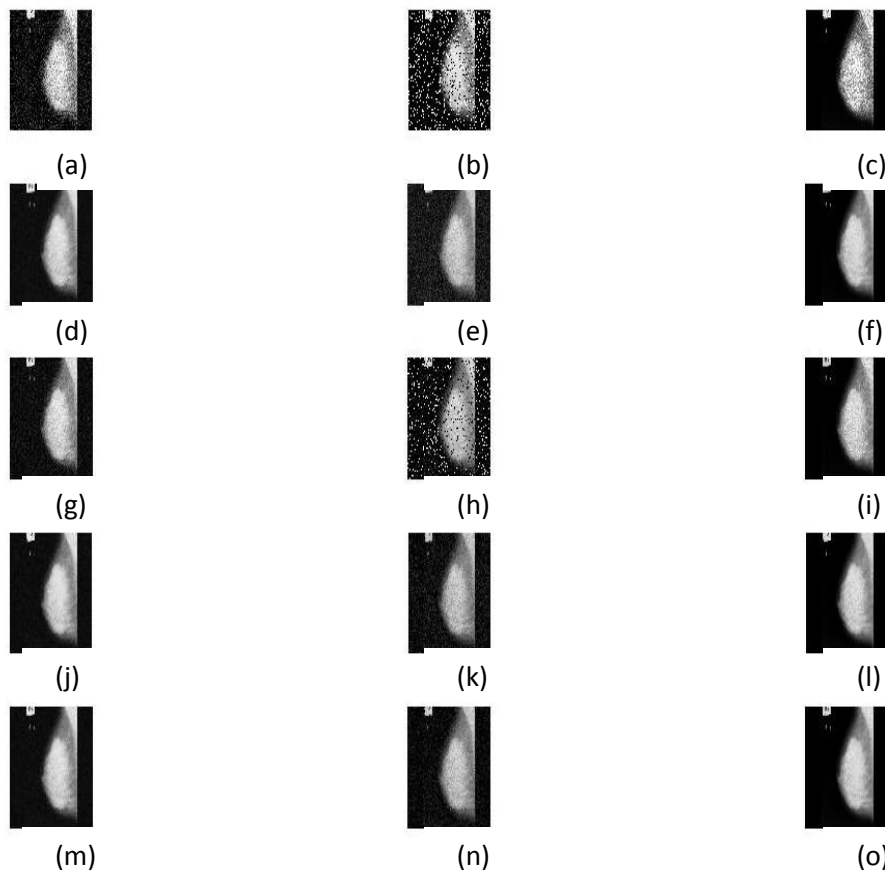


Fig 8: (a) Gaussian noise image with mean zero and variance 0.02 (b) Salt &pepper noise image with density 20% (c) Speckle noise image with variance 0.05 (d) Gaussian noise with blur (e) Salt &pepper noise with blur (f) Speckle noise with blur (g) Restored image of fig (a). (h) Restored image of fig (b). (i) Restored image of fig (c). (j) Wavelet transform and Median filter is applied to fig (g). (k) Wavelet transforms and Median filter is applied to fig (h). (l) Wavelet transform and Median filter is applied to fig (i). (m) RDTWT and Median filter is applied to fig (g). (n) RDTWT and Median filter is applied to fig (h). (o) RDTWT and Median filter is applied to fig (i).

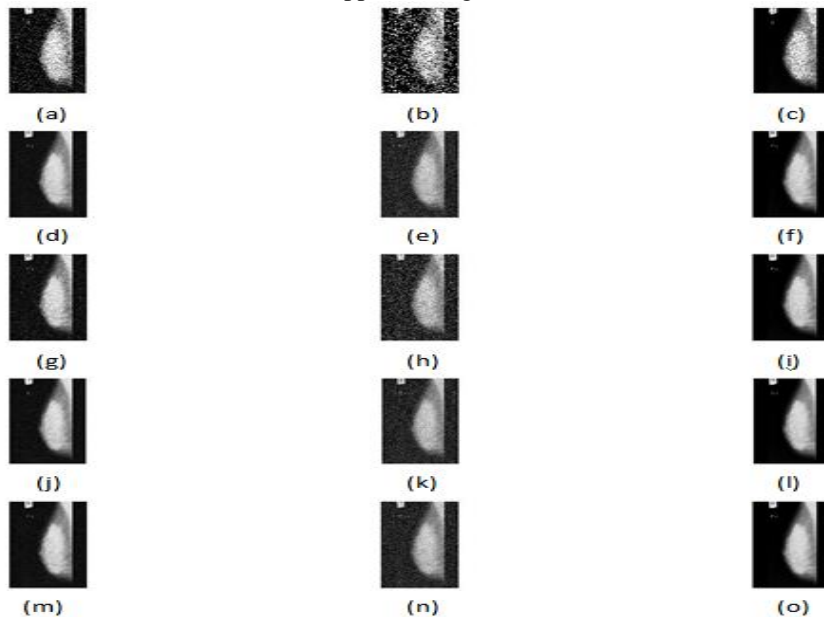


Fig 9: (a) Gaussian noise image with mean zero and variance 0.03 (b) Salt &pepper noise image with density 30% (c) Speckle noise image with variance 0.06 (d) Gaussian noise with blur (e) Salt &pepper noise with blur (f) Speckle noise with blur (g) Restored image of fig (a). (h) Restored image of fig (b). (i) Restored image of fig (c).

(c). (j) Wavelet transform and Median filter is applied to fig (g). (k) Wavelet transform and Median filter is applied to fig (h). (l) Wavelet transform and Median filter is applied to fig (i). (m) RDTWT and Median filter is applied to fig (g). (n) RDTWT and Median filter is applied to fig (h). (o) RDTWT and Median filter is applied to fig (i).

Table 1: Comparison of PSNR, MAE values of the restored and de-noised image corrupted with Gaussian blur, Gaussian noise having zero mean 0.01 variance, 10% of salt &pepper noise and speckle noise with variance 0.04.

Methods	PSNR			MAE		
	Gaussian noise	Salt&Pepper Noise	Speckle Noise	Gaussian noise	Salt&Pepper Noise	Speckle Noise
BID	36.4622	34.8249	35.9641	1.5018	2.4548	1.8820
BID+Wavelet+Median	40.3541	35.5760	37.3447	0.9111	2.0963	1.5535
BID+RDTWT+Median	40.3767	35.5668	37.3464	0.9090	2.1614	1.5535

Table 2: Comparison of PSNR, MAE values of the restored and de-noised image corrupted with Gaussian blur, Gaussian noise having zero mean 0.02 variance, 20% of salt &pepper noise and speckle noise with variance 0.05.

Methods	PSNR			MAE		
	Gaussian noise	Salt&Pepper Noise	Speckle Noise	Gaussian noise	Salt&Pepper Noise	Speckle Noise
BID	34.8286	32.8286	34.7061	2.0905	7.8193	2.3034
BID+Wavelet+Median	37.7542	31.4535	36.3730	1.2688	5.8702	1.6539
BID+RDTWT+Median	37.7766	31.6715	36.3664	1.2668	5.3133	1.6572

Table 3: Comparison of PSNR, MAE values of the restored and de-noised image corrupted with Gaussian blur, Gaussian noise having zero mean 0.03 variance, 30% of salt &pepper noise and speckle noise with variance 0.06.

Methods	PSNR			MAE		
	Gaussian noise	Salt&Pepper Noise	Speckle Noise	Gaussian noise	Salt&Pepper Noise	Speckle Noise
BID	34.0804	32.1624	35.3782	2.5646	5.3443	2.2228
BID+Wavelet+Median	36.2743	32.0388	36.1753	1.5885	4.5984	1.9554
BID+RDTWT+Median	36.2847	32.0428	36.1762	1.5861	4.5923	1.9559

VII. Conclusion And Future Scope

The proposed approach is used to restore and enhance mammographic images consists of Gaussian noise, Salt and Pepper noise, speckle noise and Gaussian blur. The hybrid combination of BID, Real dual tree wavelet transform and median filtering approach gives better result than simple BID and conventional wavelet transform approaches in case of Gaussian noise and speckle noise , in other case the Salt & pepper noise doesn't gives good result as compared to other two noises. The resultant approach gives 4% increase in PSNR and the visible quality of the mammographic image is also good for medical diagnose purpose.

References

- [1]. Rajesh kocher and shewetank arya, "Restoration of mammographic image based on BID with different Types of Noise and Gaussian Blur", International conference on advantages
- [2]. In communication, Network, and Computing, CNC .pp:825-831, 2014.
- [3]. Da-zeng T. and Ming-hu H, "Applications of Wavelet transform in medical image processing", Third International Conference on Machine Learning and Cybernetics, Shanghai, pp.1816-1821, 2004.
- [4]. Galigekr R., "Color-image processing: An Introduction with Some Medical Application-examples", International Conference on System in medicine and Design, pp.220-225, 2010.
- [5]. Huang Z; Zhang J. and Zhang C., "Ultrasound Image Reconstruction by Two-Dimensional Blind Total Variation Deconvolution", International Conference on Control and Automation, pp.1801-1806, 2009.
- [6]. P. Campisi and K. Egiazarian, "Blind Image Deconvolution Theory and Applications", CRC Press, 2006.
- [7]. K.H. Yap and L. Guan, "A Computational reinforced learning scheme to blind image deconvolution", IEEE Trans. On Evolutionary Computation, vol.6, no.1, pp.2-15, 2002.
- [8]. Seungjong Kim, Byongsok Min, Wongeun Oh and Joohung Lee, "Medical Image Enhancement Algorithm Using Edge-Based Denoising and Adaptive Histogram Stretching", International Journal of Bio-Science and Bio-Technology, vol.5, No.5, pp.25-38, 2013.
- [9]. D. Kundur and D. Hatzinakos, "Blind Image Deconvolution", IEEE Signal Processing Magazine, pp.43-64, 1996.
- [10]. Da-Zeng T. and Ming-hu H, "Applications of wavelet transform in medical image processing", Third International Conference on Machine Learning and Cybernetics, Shanghai, pp.1816-1821, 2004.
- [11]. J. Jensen, J. Mathorne, T. Gravesen, and B. Stage, "Deconvolution of in-vivo ultrasound B-mode images", ultrasound Imaging, vol.15, pp.122-133, Apr. 1993.
- [12]. Yu Chengpu, Zhang Cishen and Lihua Xie, "A Blind Deconvolution Approach to Ultrasound Imaging" IEEE Transactions on Ultrasonic Ferroelectric Frequency Control, Vol.59, pp.271-280, Feb. 2012.

- [13]. M.Kido,Y.Hirata,S.Yamada,and K.Kondo, "Automatic Restoration of X-ray photography by Esstimating Point Spread Function",ISCIT, pp.1180-1184,2010.
- [14]. A.Mencattini,M.Salmeri,R.Lojacono, and F.Caselli, "Mammographic Images Enhancement and Denoising for Microcalcification Detection Using Dyadic Wavelet Processing",Instrumentation and Measurement Technology Conference Sorrento,pp.49-53,April 2006.
- [15]. Ma. Guadalupe Sanchez, Vicente Vidal, Gumersindo Verdu,Patricia Mayo and Francisco Rodenas, "Medical Image Restoration With Different Types of Noise",International Conference of the IEEE EMBS,pp.4382-4385,2012. ,
- [16]. A.Grossmann, and J.Morlet, "Decomposition of hardy functions into square integrable wavelets of constant shape",SIAM J.Math.Anal,Article(CrossRef Link),Vol.15,pp.723-736,1984.
- [17]. S.Mallat, "A theory for multiresolution signal decomposition:the wavlet representation",IEEE Trans. On pattern Analysis and Machine Intelligence,Article(CrossRef Link),vol.11,pp.674-693,1989.